



ISSN: 0067-2904

Noise Reduction, Enhancement and Classification for Sonar Images

Noor H. Resham¹, Heba Kh. Abbas¹, Haidar J. Mohamad^{2*}, Anwar H. Al-Saleh³

¹Department of Physics, College of Science for Women, University of Baghdad, Baghdad, Iraq

²Department of Physics, College of Science, Mustansiriyah University, Baghdad, Iraq

³Department of Computer Science, College of Science, Mustansiriyah University, Baghdad, Iraq

Received: 18/1/2021

Accepted: 7/6/2021

Abstract

Ultrasound imaging has some problems with image properties output. These affects the specialist decision. Ultrasound noise type is the speckle noise which has a grainy pattern depending on the signal. There are two parts of this study. The first part is the enhancing of images with adaptive Weiner, Lee, Gamma and Frost filters with 3x3, 5x5, and 7x7 sliding windows. The evaluated process was achieved using signal to noise ratio (SNR), peak signal to noise ratio (PSNR), mean square error (MSE), and maximum difference (MD) criteria. The second part consists of simulating noise in a standard image (Lina image) by adding different percentage of speckle noise from 0.01 to 0.06. The supervised classification based minimum distance method is used to evaluate the results depending on selecting four blocks located at different places on the image. Speckle noise was added with different percentage from 0.01 to 0.06 to calculate the coherent noise within the image. The coherent noise was concluded from the slope of the standard deviation with the mean for each noise. The results showed that the additive noise increased with the slide window size, while multiplicative noise did not change with the sliding window nor with increasing noise ratio. Wiener filter has the best results in enhancing the noise.

Keywords: Ultrasound noise, Enhancement, Classification, simulating noise, image processing

تقليل، تحسين وتصنيف الضوضاء لصور السونار

نور حسن رشم¹، هبة خضير عباس¹، حيدر جواد محمد^{2*}، أنوار حسن الصالح³

¹ قسم الفيزياء، الكلية العلوم للبنات، جامعة بغداد، بغداد، العراق

² قسم الفيزياء، الكلية العلوم، الجامعة المستنصرية، بغداد، العراق

³ قسم الحاسبات، الكلية العلوم، الجامعة المستنصرية، بغداد، العراق

الخلاصة

تواجه تقنية التصوير بالموجات فوق الصوتية بعض المشكلات في إخراج خصائص الصورة. هذه المشاكل تؤثر على قرار الاختصاصي. إن نوع ضوضاء الموجات فوق الصوتية هو ضوضاء البقع التي لها نمط محبب يعتمد على الإشارة. هناك جزئين من هذه الدراسة: الجزء الأول هو تحسين الصور باستخدام فلاتر Weiner و Gamma و Lee و Frost المتكيفة مع نافذة انزلاقية 3x3 و 5x5 و 7x7. تقييم الكفاءة للفلاتر تم باستخدام معايير نسبة الإشارة إلى الضوضاء (SNR)، ونسبة قمة الإشارة إلى الضوضاء (PSNR)،

*Email: dr.bassmahussain@kus.edu.iq

ومتوسط الخطأ التربيعي (MSE)، الفرق الأكبر (MD). يتضمن الجزء الثاني محاكاة الضوضاء بالصورة القياسية (صورة Lina) عن طريق إضافة ضوضاء البقع بنسبة مئوية من 0.01 إلى 0.06. الحد الأدنى للمسافة القائم على التصنيف الخاضع للإشراف المستخدم لتقييم النتائج تم استخدامه على أربعة مربعات موجودة في مواقع مختلفة من الصورة. تمت إضافة ضوضاء البقع بنسبة مئوية من 0.01 إلى 0.06 لحساب الترابط داخل الصورة. تم استنتاج الضوضاء المترابطة عن طريق استخدام منحدر الانحراف المعياري بمتوسط كل ضوضاء. أظهرت النتائج أن الضوضاء الجمعية تزداد مع حجم النافذة المنزقة، بينما الضوضاء الضريبية لا تتغير مع النافذة المنزقة ولا تزداد مع زيادة نسبة الضوضاء. مرشح Wiener له نتائج أفضل في تحسين الضوضاء..

1. Introduction

As a modality for medical diagnosis, ultrasonic imaging is commonly used in clinical practice. While diagnostic ultrasound is considered a harmless technique, anatomical scanning enables real-time and non-invasive scanning. The speckle artefact that results from destructive interference effects between returned echoes pervades the B-mode images. This artefact presents fine-false structures that are beyond the capacities of the imaging system for apparent resolution. This reduces the contrast of the image and covers the actual borders of the tissue under investigation [1]. Its occurrence can significantly compromise the efficacy of the diagnosis, which introduces a high degree of subjectivity in the interpretation of the images [2].

Speckle is a dual noise that in ultrasound and Synthetic Aperture Radar (SAR) decreases image quality and visual assessment. In the broad variety of imaging applications described above, this involves robust dandruff removal techniques. In recent years, Despeckle's filtration applications have been a rapidly emerging area of study. For all those employed in medical imaging techniques and ultrasound and video image processing and analysis, this work is significant [3,4]. It provides researchers, biomedical engineers, computer engineers and medical imaging engineers with different levels of materials interested in developing better quality images and minimizing speckle-noise damage [5,6]. In the sense that it is a deterministic artefact, Speckle differs from other forms of noise, which means that two signals or two images obtained under the same conditions will undergo the same pattern of spot damage. If any or all of the conditions vary, the pattern of spot damage will be different. Digital image processing consists of calculations that transform one image into another in which particular details of interest are highlighted and/or dilutes or eliminates details that are not important to the application [7].

Several scientific studies have dealt with this area, some of which are chosen because of their proximity to the field of study. Diwakar *et al.*, in 2018 [8], studied original noisy CT images in the Shearlet domain using the Bayes shrinkage law. The proposed framework contrasted with existing methods and it was noted that the performance of the proposed system was superior to the visual quality, Image Quality Index (IQI) and Peak Signal-to-Noise Ratio (PSNR) performance of existing methods. The proposed work was shown by experimental evaluation to: (i) effectively removing the noise in CT images, (ii) preserving the edge and structural information, and (iii) retaining clinically relevant data. In 2019, Choi and Jeong [9] proposed a new algorithm based on speckle reducing anisotropic (SRAD) and Bayesian threshold in the wavelet field. In this algorithm, SRAD was used as a pre-processing filter, and Bayes threshold was used to remove residual noise in the resulting image. Compared with conventional filtering techniques, the experimental results showed that the proposed algorithm showed superior performance in terms of peak signal-to-noise ratio (mean = 28.61 dB) and structural similarity (mean = 0.778). In 2020, Duarte-Salazar *et al.* [10], gave description of 27 techniques primarily focused on smoothing or eliminating spot noise in medical ultrasound images. They highlighted the importance of improving smoothness and

removing noise that is directly related to many processes (such as detection of areas of interest). Conducting assessments and analysis with a wide scope determines where conventional techniques such as spatial filtering, diffusion filtering, and wavelet filtering are defined. Describe modern machine learning techniques that rely on deep learning in the field of spot noise filtering, as well as modern and hybrid models. Five full reference distortion (FR) scales, popular in candidate assessments, are used along with the technique of compensation between FR and non-reference (NR) scales. It can provide greater certainty in the classification of filters by looking at their behaviour details in terms of the perceptual consistency offered by the NR scales.

In this study, two images were collected from the Government hospital for breast and abdominal muscles. This study consists of two parts. The first part used four enhancing filters namely Weiner, Lee, Gamma and Frost. These filters have a different sliding window (3x3, 5x5, 7x7). The evaluation process depends on MSE, SNR, PSNR, and MD. The second part consists of simulating the speckle noise with a different ratio in the standard image (Lena). Then a classification process achieved by choosing different blocks located in the image is presented. Mean (σ) and standard deviation (SD) were calculated for these blocks at different noise ratio. The coherent noise was calculated from the slope of the SD/ σ for each noise.

2. Theoretical concepts

Speckle Noise

It is crucial to have an accurate and reliable model to perfect the denoising methods. This is not a simple task; the following model is, however, considered a good model for speckle noise images [11]:

$$w(x, y) = s(x, y) \times n_m(x, y) + n_a(x, y) \quad (1)$$

Since additive noise is considered to be lower than multiplicative noise, Loupas, McDicken and Allan, in 1989[12] proposed the following signal-dependent noise model for speckle specification in ultrasound images:

$$w(x, y) = s(x, y) \times n_m(x, y) \quad (2)$$

One of significant topics in the processing of the wall is to analyze the noise that suffers from noise. many algorithms are used to remove noise from the image, the best of which is to remove noise from the image while preserving fine details. There are fast and efficient linear noise removal methods, but they do not preserve image detail. Therefore, the noise removal filters are classified into the following categories: (1) Non-adaptive filters: - These filters take the entire image signal parameters into consideration and leave the non-public characteristics of the image. (2) Adaptive Filters: - These filters provide changes in the local properties of the image texture along with the nature of the sensor. Many filters were used to remove noise which applied in this work [13-15]:

Wiener Filter

The Wiener filter is a linear filter. The Wiener filtering method needs information on the noise spectrum and the original image to be assumed. Signal and additive noise are stationary linear with known spectral properties. It is known as autocorrelation and cross-correlation [13].

2. Lee Filter

Many methods for speckle de-noising have been proposed. The most common adaptive methods designed so far are Lee [14], Frost [15].

Lee filter (also called Lee MMSE filter) is based on linear speckle noise model and the utilization of minimum mean square error (MMSE) criterion. Image data enhancement is then based on the filter equation:

$$\hat{R}(t) = W(t) + \bar{I}(t)[I(t) - W(t)] \quad (3)$$

$\hat{R}(t)$ the de-noised image, $I(t)$ image with speckle noise, $\bar{I}(t)$ the mean image intensity within the filter window, and $W(t)$ weighted coefficient determined as:

$$W(t) = 1 - \frac{c_u^2}{c_I^2(t)} \quad (4)$$

where c_u and $c_I(t)$ are variation coefficients of speckle $u(t)$ and image $I(t)$ respectively:

$$c_u = \frac{\sigma_u}{u}; \quad c_I(t) = \frac{\sigma_I(t)}{\bar{I}(t)} \quad (5)$$

Gamma Filter

Special low-pass filters, called Gamma filters, can preserve image details by filtering on individual pixels in an image using the gray-level values in a square window surrounding each pixel, and NLOOK is the number of looks. The form of the Gamma filter expressed as [16].

$$D = I^2 \times B \times B + 4 \times ALFA \times NLOOK \times I \times CP \quad (6)$$

for $C_u < C_i < C_{max}$, $R = CP$ for C_i greater than or equal to C_{max} . where: CP is center pixel gray-level value, I is mean gray level in the filter window, $C_u = 1/\text{SQRT}(NLOOK)$, $C_i = \text{SQRT}(\text{VAR}) / I$, $C_{max} = \text{SQRT}(2) \times C_u$, $ALFA = (1 + C_u^2) / (C_i^2 - C_u^2)$, B is $ALFA - NLOOK - 1$, where VAR is variance in filter window

Frost filter

Frost filter is an adaptive filter that convolves pixels in a fixed window with impulse response $m(t)$ given by the equation:

$$m(t) = \exp(-K \cdot c_I(t) \cdot |t_0|) \quad (7)$$

where K is the filter parameter and $|t_0|$ is the distance measures from pixel located at coordinates t .

Image quality evaluation

There are objective evaluations for judging the effect of noise reduction. The evaluation of the quality of the performance of each filtering method is the differences between the original image $g(x, y)$ and the filtered image $f(x, y)$. This is quantified by many parameters such as [17-19]:

1. Signal- to- Noise Ratio (SNR)

Signal to noise ratio of an image is calculated as:

$$SNR = 10 \log_{10} \sum_{x=1}^m \sum_{y=1}^n \frac{f(x, y)^2}{(f(x, y) - g(x, y))^2} \quad (8)$$

where $f(x, y)$ is pure ideal image not polluted by noise, $g(x, y)$ is captured image polluted by noise, m and n are the image size. The bigger the SNR the better the noise reduction effect. The SNR has been proved to be a very sensitive test for image degradation but is completely non-specific. Any small change in image noise by despeckling would cause an increase in the SNR.

2. Peak Signal to Noise Ratio (PSNR)

PSNR is the peak signal-to-noise ratio in decibels (dB). The PSNR is only meaningful for data encoded in terms of bits per sample, or bits per pixel.

$$PSNR = 10 \log_{10} \sum_{x=1}^m \sum_{y=1}^n \frac{m \times n \times 255 \times 255}{(f(x, y) - g(x, y))^2} \quad (9)$$

Also the bigger PSNR the better the noise reduction effect.

3. Mean Square Error (MSE)

The MSE is expressed by:

$$MSE = \frac{1}{m \times n} \sum_{x=1}^m \sum_{y=1}^n ((f(x, y) - \hat{g}(x, y))^2) \quad (10)$$

where $\hat{g}(x, y)$ is processed image after noise reduction from noise polluted image $g(x, y)$ and it should be smaller for better noise reduction. The MSE has been widely used to quantify image quality. When it is used alone, it does not correlate strongly enough with perceptual quality. It should be used together with other quality metrics and visual perception.

Maximum Difference (MD)

Maximum difference measure is defined as:

$$MD = \max\left(\sum_{x=1}^m \sum_{y=1}^n |f(x, y) - g(x, y)|\right) \quad (11)$$

Simulation using supervised classification technique

Simulation is a virtual representation of reality. It may also be defined as the process of knowing the characteristics and exhibiting the behaviour of a particular physical system. Sometimes a learner finds it quite difficult to understand any physical system behaviour by just reading it from the written material, but once he can see the things happening on the computer system the things change. That is why real-life techniques of image enhancement are important. In this study, the importance of simulation techniques in the field of digital image processing is presented. This was achieved by conducting simulations to implement basic image improvement techniques. Different values of speckle-noise were added to the real images. Then, the supervised classification technique based on the minimum distance method was applied by selecting several blocks. Lastly, both the mean and the standard deviation of the block was calculated to find the degree of coherent (slope) that represents the ratio between the standard deviation and the mean [20].

• Supervised Classification

In supervised classification, the user or image analyst “supervises” the pixel classification process. One of the supervised classification algorithms is the Minimum Distance method. It uses the mean vectors for each class and calculates the Euclidean distance from each unknown pixel to the mean vector for each class. The pixels are classified to the nearest class. The image element due to the vector data dimension I and base the minimum distance MD are given by the following:

$$M_D = (I(x, y) - \mu) \quad (12)$$

The method is calculating the mean μ for each class and finds the distance between each pixel to class mean vector. Then allocate each pixel to the class it is closest to [21].

• Statistical Mean (μ)

The mean of a data set is simply the arithmetic average of the values in the set obtained by summing the values and dividing by the number of values. The mean distribution represents by [22]:

$$\mu = \frac{1}{mn} \sum_{x=1}^m \sum_{y=1}^n I(x, y) \quad (13)$$

where n , m row and column image, respectively, I express the original image (one band or multi bands).

• Standard Deviation (σ):

The standard deviation (σ), which is the square root of the variance, reflects the spread in the data. Thus, a high contrast image will have a larger variance, and a low contrast image will have a low variance. It indicates the closeness of the fused image to the original image I at a pixel level. The ideal value is zero [21].

$$\sigma = \sqrt{\frac{\sum_{x=1}^m \sum_{y=1}^n (I(x, y) - \mu)^2}{m \times n}} \quad (14)$$

• Number of Lucks

Slope represents the ratio between standard deviation and mean as [23, 24]:

$$\text{slop} = \frac{\sigma}{\mu} \quad (15)$$

3. Ultrasound Images

The tested images were two, represented in Figure 1 collected from Yarmook Government Hospital-Baghdad. It was chosen according to the difference between them in skin depth. Figure 1 (a) is a breast ultrasound image size 284x187 pixel with pixel depth is 24 bit. Figure 1 (b) shows abdominal muscles for a person who needs treatment with size 527x104 pixel and pixel depth 24 bit.

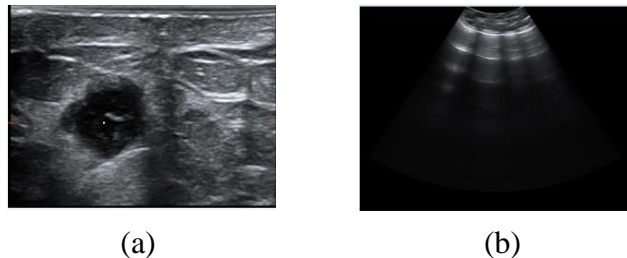


Figure 1-Ultrasound images used in the study (a) Breast (b) abdominal muscles.

4. Results and analysis

This study consists of two parts. The first part includes enhancement of the ultrasound images using filters (wiener, Lee, Gamma, and Frost) with filter size 3x3, 5x5 and 7x7. The second part includes the simulation process by adopting real images and applying the classification technique after adding percentages of speckle noise.

Enhancement

The enhancement process was applied directly using Weiner and Gamma filters for the tested images shown in Figure 2. It was noticeable that the noise enhancement was the same for all noise per cent in the 3x3 sliding window for both Weiner and Gamma filters for all noise ratio. The same is for sliding window 5x5 and 7x7 the noise was the same in the image.

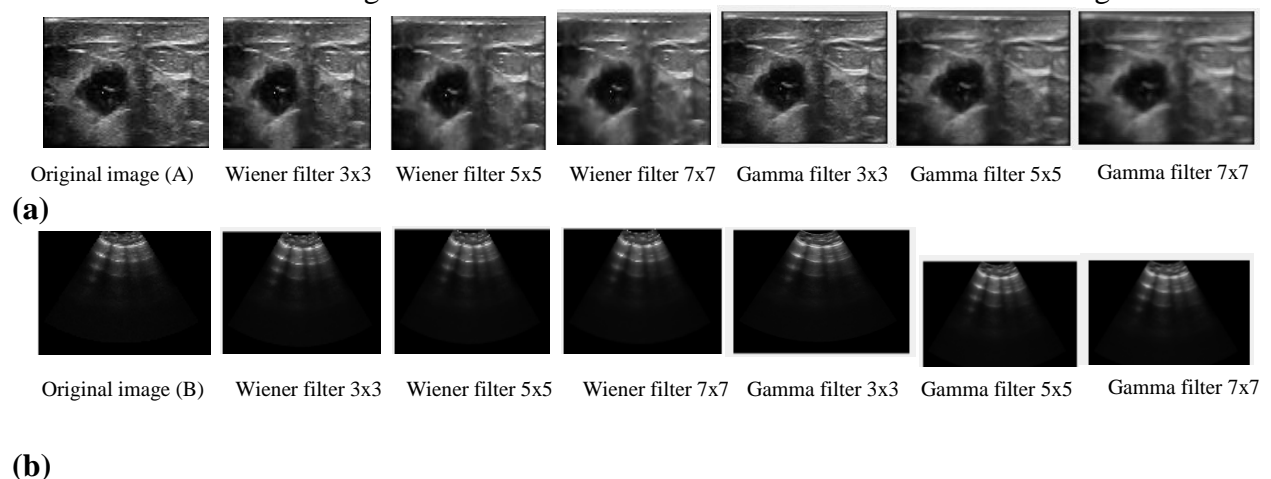


Figure 2-Wiener and Gamma filters with different mask size for the (a) A-image, (b) B-image.

Table 1 represents the mean value for the additive and multiplicative noise for both Wiener and Gamma filters. It has an indicator for Gamma filter in decreasing mean value with increase window size in the additive noise (which is the behaviour of this type of noise). Multiplicative noise does not change with increasing the noise or the filter window size.

Table 1- The noise values for the Wiener and Gamma filters with different window size.

| Images | size | Wiener filter | Gamma filter | Wiener filter | Gamma filter |
|---------|------|---------------------|---------------------|---------------------------|---------------------------|
| | | Mean additive noise | Mean additive noise | Mean multiplicative noise | Mean multiplicative noise |
| Image A | 3×3 | -0.0570 | 0.01235 | 0.9887 | 0.9882 |
| | 5×5 | -0.1646 | 0.1447 | 0.9698 | 0.9767 |
| | 7×7 | -0.1531 | 0.3570 | 0.9643 | 0.9786 |
| Image B | 3×3 | -0.0017 | 0.2087 | 0.5555 | 0.5582 |
| | 5×5 | -0.0100 | 0.3699 | 0.5494 | 0.5576 |
| | 7×7 | -0.0121 | 0.4430 | 0.5409 | 0.5546 |

The Frost and Lee filters results are shown in Figure 3 and 4 for the additive and multiplicative noise. The size of the window for both filters is presented to show the difference of the noise output. The noise value with the filter window size had a noticeable effect on the results and this is discussed in conclusion.

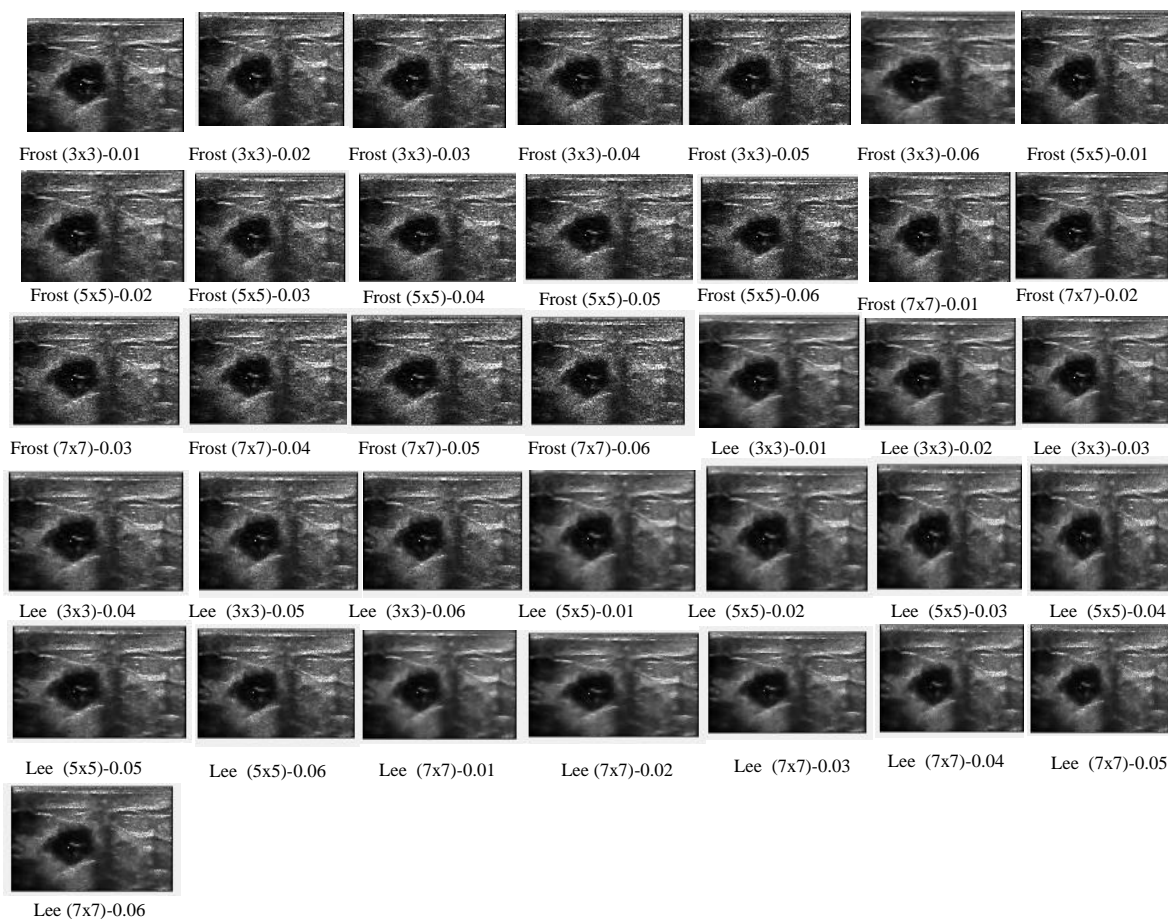


Figure 3-Image A enhancement of Frost and Lee filters with different mask window and noise values.

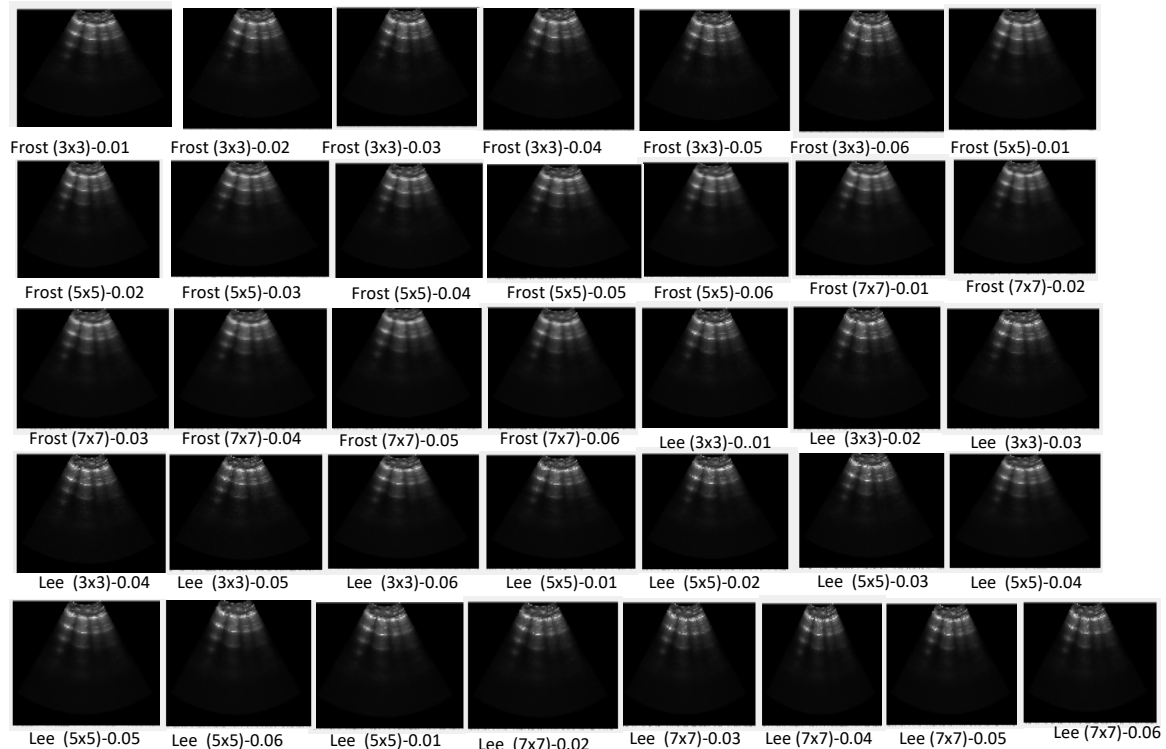


Figure 4-Image B enhancement of Frost and Lee filters with different mask window and noise values.

The summary values of the quantitative criteria for the additive and multiplicative noise are tabulated in Table 2. Table 2 shows the size of the windows of the Frost and Lee filters for image A and B.

Table 2- The noise values for the Frost and Lee filters with different window size.

| Image A | | Frost filter | | Lee filter | | |
|---------|-------|---------------------|---------------------------|------------|---------------------|---------------------------|
| | Noise | Mean additive noise | Mean multiplicative noise | | Mean additive noise | Mean multiplicative noise |
| (3x3) | 0.01 | 0.3613 | 0.9756 | (3X3) | -0.0566 | 0.9877 |
| | 0.02 | 0.3120 | 0.9763 | | 0.0298 | 0.9893 |
| | 0.03 | 0.4393 | 0.9778 | | 0.0296 | 0.9910 |
| | 0.04 | 0.4513 | 0.9800 | | 0.0754 | 0.9943 |
| | 0.05 | 0.3872 | 0.9801 | | 0.1631 | 0.9961 |
| | 0.06 | 0.5572 | 0.9841 | | 0.0852 | 0.9970 |
| (5X5) | 0.01 | 0.5456 | 0.9746 | (5X5) | 0.0041 | 0.9695 |
| | 0.02 | 0.4898 | 0.9745 | | 0.0259 | 0.9695 |
| | 0.03 | 0.5295 | 0.9754 | | 0.0324 | 0.9716 |
| | 0.04 | 0.5625 | 0.9765 | | -0.0442 | 0.9709 |
| | 0.05 | 0.6401 | 0.9769 | | 0.1001 | 0.9748 |
| | 0.06 | 0.6143 | 0.9777 | | 0.1153 | 0.9768 |
| (7X7) | 0.01 | 0.6135 | 0.9737 | (7X7) | 0.0941 | 0.9639 |
| | 0.02 | 0.5968 | 0.9732 | | 0.0289 | 0.9637 |
| | 0.03 | 0.7160 | 0.9749 | | -0.0189 | 0.9638 |
| | 0.04 | 0.5979 | 0.9741 | | 0.0318 | 0.9657 |
| | 0.05 | 0.7302 | 0.9753 | | 0.1187 | 0.9671 |
| | 0.06 | 0.5986 | 0.9739 | | 0.1609 | 0.9704 |
| Image B | | Frost filter | | Lee filter | | |

| | Noise | Mean additive noise | Mean multiplicative noise | | Mean additive noise | Mean multiplicative noise |
|-------|-------|---------------------|---------------------------|-------|---------------------|---------------------------|
| (3×3) | 0.01 | 0.3613 | 0.9756 | (3X3) | -0.0566 | 0.9877 |
| | 0.02 | 0.3120 | 0.9763 | | 0.0298 | 0.9893 |
| | 0.03 | 0.4393 | 0.9778 | | 0.0296 | 0.9910 |
| | 0.04 | 0.4513 | 0.9800 | | 0.0754 | 0.9943 |
| | 0.05 | 0.3872 | 0.9801 | | 0.1631 | 0.9961 |
| | 0.06 | 0.5572 | 0.9841 | | 0.0852 | 0.9970 |
| (5X5) | 0.01 | 0.5456 | 0.9746 | (5X5) | 0.0041 | 0.9695 |
| | 0.02 | 0.4898 | 0.9745 | | 0.0259 | 0.9695 |
| | 0.03 | 0.5295 | 0.9754 | | 0.0324 | 0.9716 |
| | 0.04 | 0.5625 | 0.9765 | | -0.0442 | 0.9709 |
| | 0.05 | 0.6401 | 0.9769 | | 0.1001 | 0.9748 |
| | 0.06 | 0.6143 | 0.9777 | | 0.1153 | 0.9768 |
| (7X7) | 0.01 | 0.6135 | 0.9737 | (7X7) | 0.0941 | 0.9639 |
| | 0.02 | 0.5968 | 0.9732 | | 0.0289 | 0.9637 |
| | 0.03 | 0.7160 | 0.9749 | | -0.0189 | 0.9638 |
| | 0.04 | 0.5979 | 0.9741 | | 0.0318 | 0.9657 |
| | 0.05 | 0.7302 | 0.9753 | | 0.1187 | 0.9671 |
| | 0.06 | 0.5986 | 0.9739 | | 0.1609 | 0.9704 |

The Frost filter showed an increase of the additive noise with increasing the window size filter, and it decreased by increasing the noise ratio of the image. Moreover, its value is higher than the Wiener and Gamma filters.

Figure 5 represents the additive and multiplicative noise for Weiner and Gamma filters. The behaviour of the noise in the image is noticeable from the diagram. Wiener filters showed lower noise range comparing with the Gamma filter.

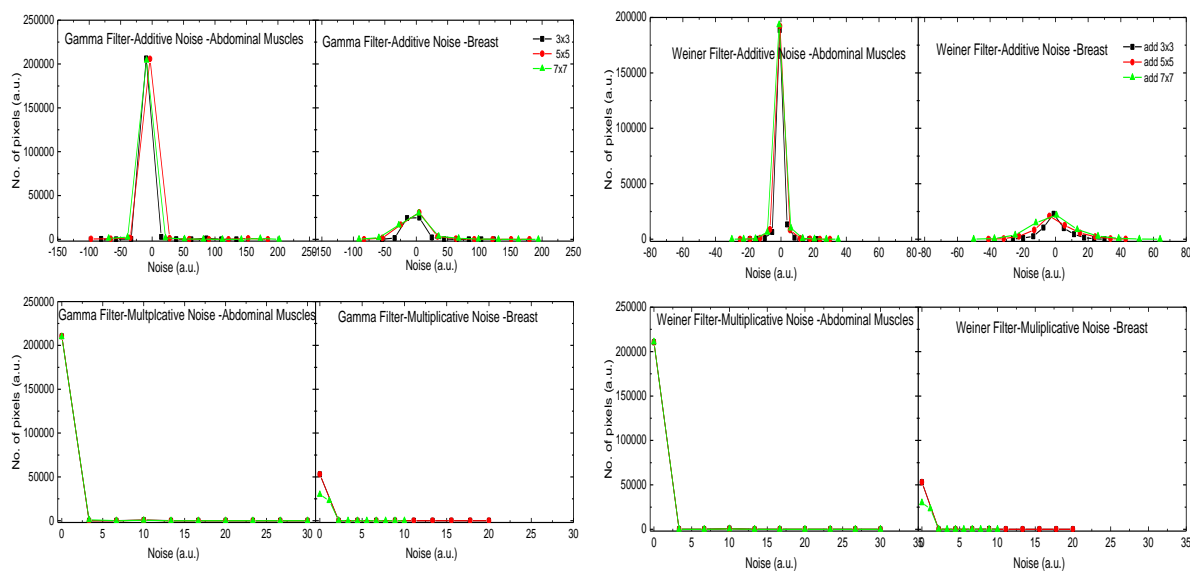


Figure 5-Additive and multiplicative noise for Weiner and Gamma filters for both image A and B

Figure 6 shows the additive and multiplicative noise for Frost and Lee filters. The plot arranges the noise per cent over each other to show the effect of the filters. Moreover, the noise in the image was higher than that of the other filters. The advantages of Frost filter are that the multiplicative noise was lower than the that of the other filters and decreased with increasing the window filter size.

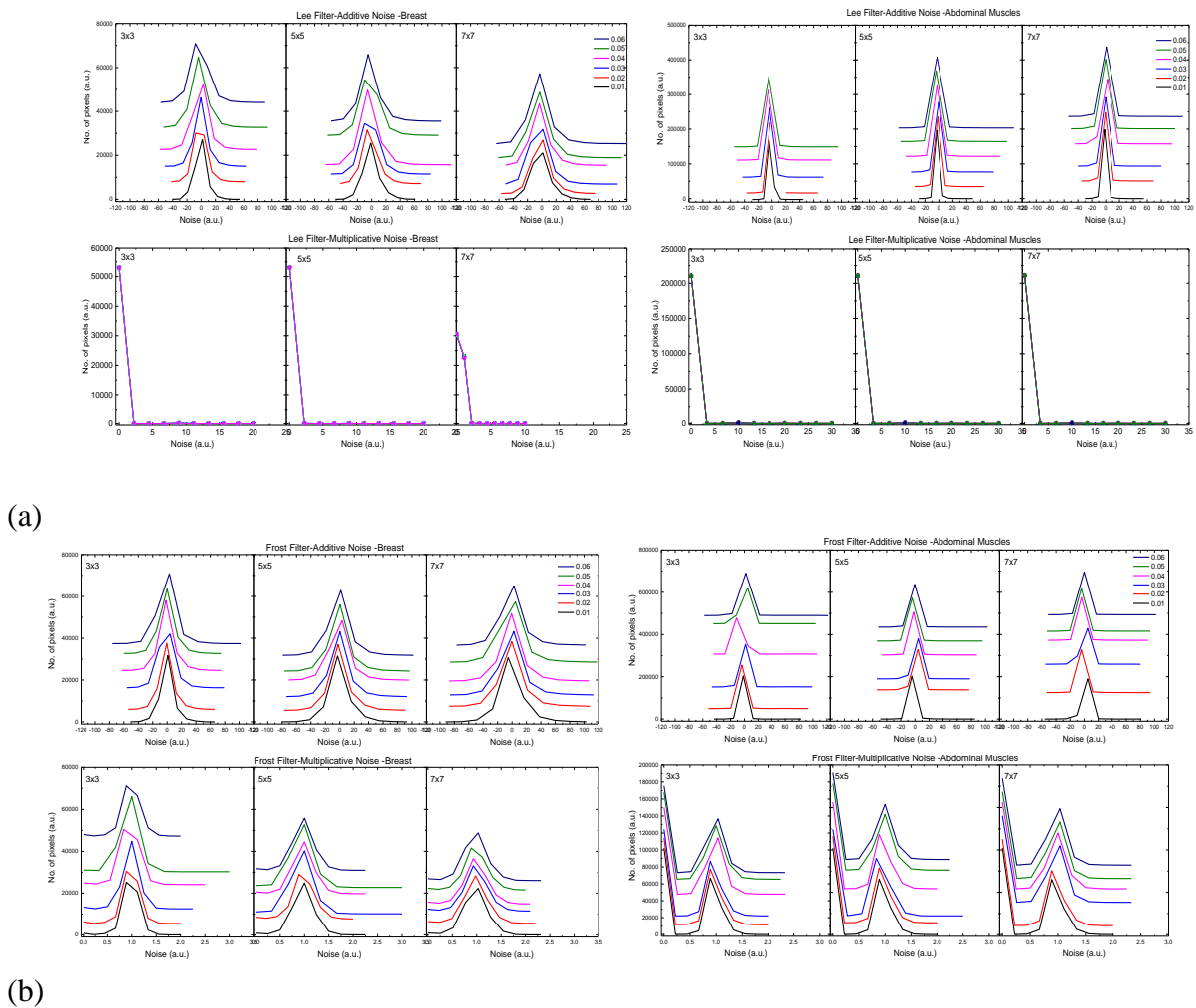


Figure 6-Additive and multiplicative noise for (a) Lee and (b) Frost and filters for both image A and B

Results evaluation

The filters were evaluated using four criterions namely MSE, SNR, PSNR, and MD. The results are presented in Figure 7 and shows that: Wiener has the lowest value of MSE, Gamma showed the lowest value of PSNR, Frost recorded the lowest value of SNR. The MD criteria showed that Gamma filter had the lowest values.

From Figure 7, it can be concluded that the best filter was Wiener with window size 3x3, then the next filter is Lee. While the worst filters were Gamma and Frost. However, Frost filter results in the multiplicative noise had the lowest values.

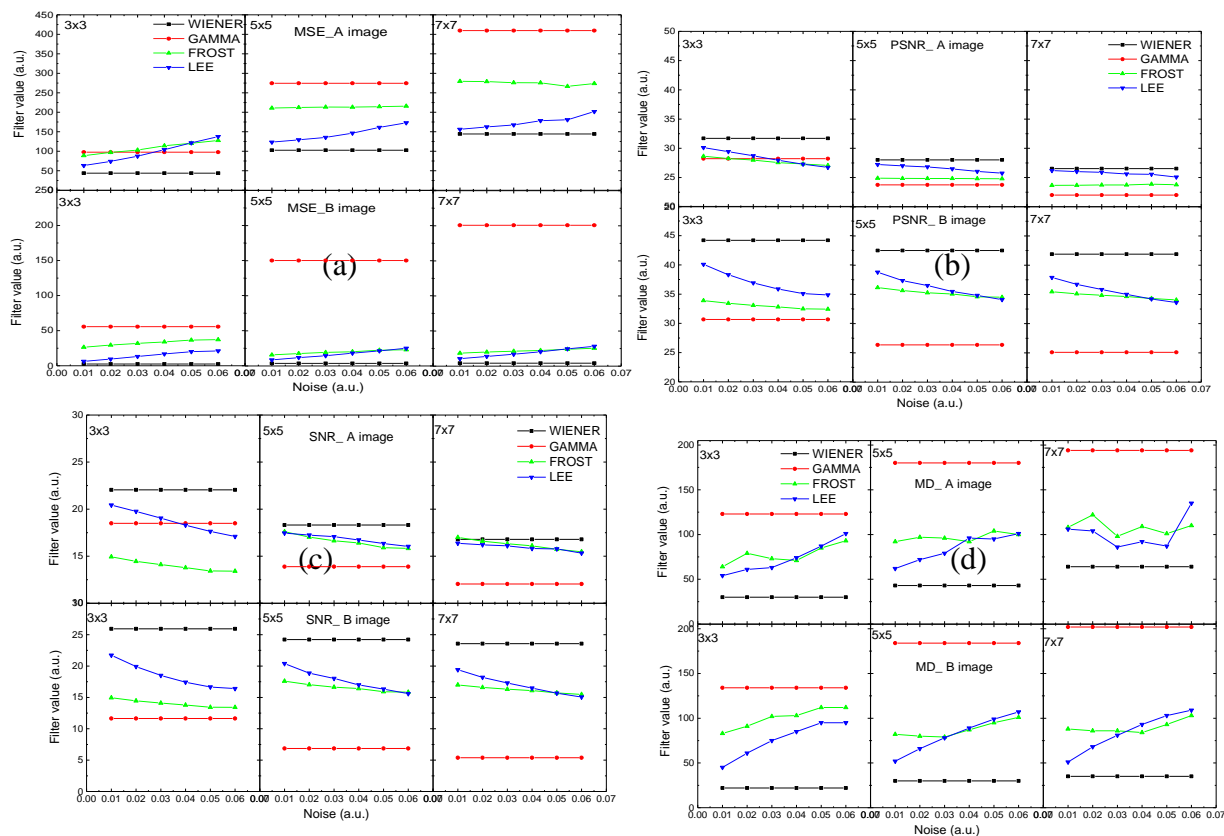
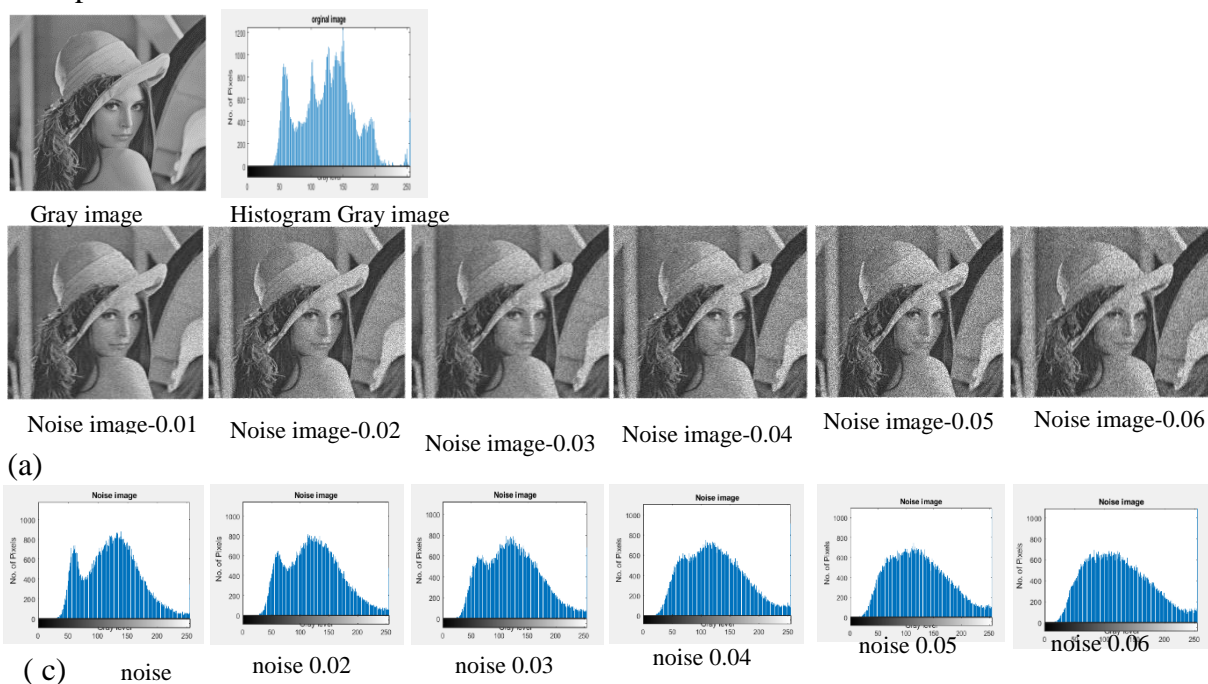


Figure 7-The filters quality with different window size in (a) MSE (b)PSNR, (c) SNR, and (d) MD criterion for both tested images.

Noise was simulated within the standard image (Lena) which is without any noise as presented in Figure 8. The same values of the noise were added to the Lena image and a histogram was plotted to check the noise behaviour for the additive and multiplicative noise. The change was obvious for the image when increasing the noise value which can be seen in the histogram. The same procedure is presented for the Lena image for the additive and multiplicative noise.



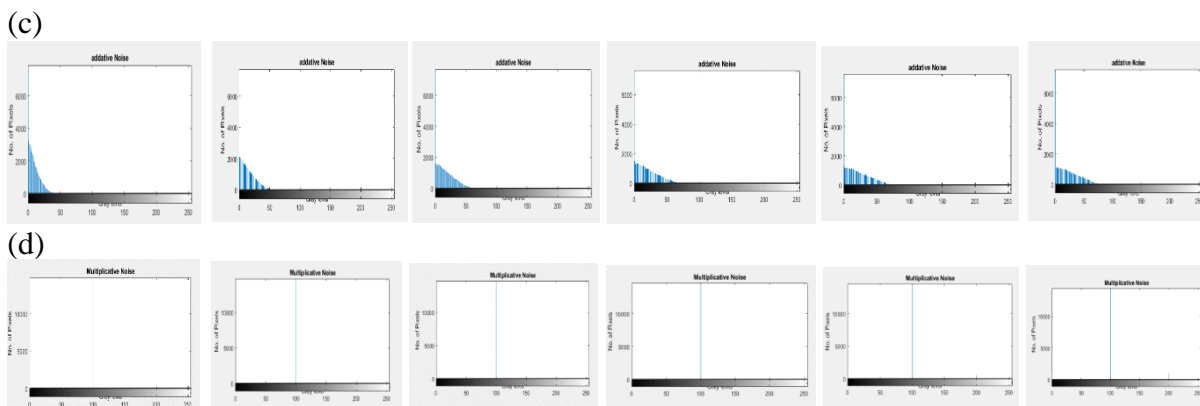


Figure 8-The standard image with the associated histogram and (a) image with noise, (b) image histogram with noise, (c) additive histogram with noise and (d) multiplicative histogram with noise.

Four blocks of different locations were chosen manually within the image. Statistical criteria, like mean and standard deviation, were calculated for these four blocks. The same position, of the blocks, were considered to measure the noise for different noise ratio. The block locations are as dispatched in Figure 9.

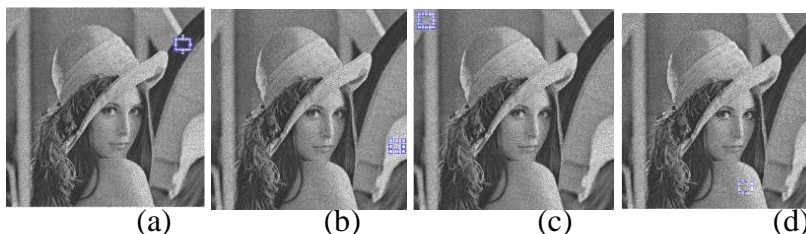


Figure 9-The block locations used within this study for different locations.

The slope from equation 16 is plotted in Figure 10 for the mean and standard deviation for each noise ratio.

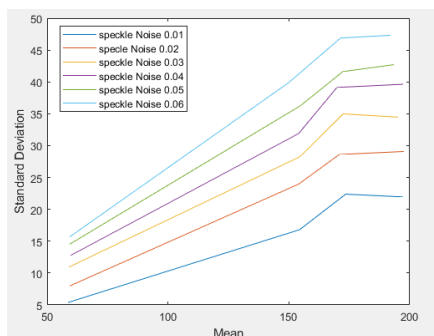


Figure 10-The relationship between standard deviation and mean for each speckle noise. Table 3 shows the slope behaviour for coherent noise, which increased by increasing the noise ratio. This means that the number of luck has increased with increasing the noise in the image which means that the distortion in the image has increased. This is considered as an indicator of the noise level in the image.

Table 3- Statistical criteria’s speckle noise for Lena image

| Speckle noise images | classes | Mean | Standard deviation | Slope |
|----------------------|---------|----------|--------------------|-------|
| 0.01 | a | 58.6042 | 5.3851 | 0.12 |
| | b | 154.4386 | 16.8117 | |
| | c | 173.4887 | 22.3888 | |
| | d | 197.1531 | 21.9540 | |

| | | | | |
|------|---|----------|---------|------|
| 0.02 | a | 59.5000 | 8.0104 | 0.16 |
| | b | 154.0386 | 23.9680 | |
| | c | 170.8622 | 28.6160 | |
| | d | 197.6688 | 29.0880 | |
| 0.03 | a | 58.9410 | 10.9312 | 0.18 |
| | b | 154.5789 | 28.2697 | |
| | c | 172.4386 | 34.9880 | |
| | d | 195.2406 | 34.4719 | |
| 0.04 | a | 59.7465 | 12.7783 | 0.20 |
| | b | 154.0386 | 31.9032 | |
| | c | 169.8546 | 39.1395 | |
| | d | 197.3406 | 39.6390 | |
| 0.05 | a | 59.3438 | 14.5388 | 0.22 |
| | b | 154.6807 | 36.2452 | |
| | c | 172.3033 | 41.6239 | |
| | d | 193.7156 | 42.7286 | |
| 0.06 | a | 59.5174 | 15.7345 | 0.25 |
| | b | 149.8561 | 39.8785 | |
| | c | 171.3960 | 46.9014 | |
| | d | 192.1688 | 47.3277 | |

Conclusion

The behaviour of the speckle noise in the ultrasound images was presented and evaluated using different criteria. The simulated noise in the Lena image gave a good indicator so as to remove the noise and evaluate the presented filters. It was concluded that one way of calculating noise in the image is by calculating the coherent value in the image from the mean and standard deviation criteria.

The filters have different behaviour with the multiplicative and additive noise that were added to the image. The multiplicative noise increased with filter window size, while the multiplicative noise was not affected by the filter window size.

The additive noise, using Lee filter, increased with increasing the window size and the added noise ratio. However, its values are less than Frost and Gamma filters. Wiener and Lee filters had the lowest values in the additive noise. While Frost filter had the lowest values in the multiplicative noise as compared with the other filters.

The filtering behaviour changes according to the image type. The image of ultrasound changes according to the human tissue or human body location under study. Therefore, the response of the filter changes accordingly. This was noticed from the additive and multiplicative noise scale output.

References

- [1] Mr. Mandar D. Sontakke and Dr. Mrs. Meghana S. Kulkarni, "Different Types of Noises In Images And Noise Removing Technique", *International Journal of Advanced Technology in Engineering and Science*, vol. 3, no. 1, pp. 102-115, 2015.
- [2] H. Ibrahim, "Adaptive switching median filter utilizing quantized window size to remove impulse noise from digital images Asian Transactions on Fundamentals of Electronics", *Communication & Multimedia*, vol. 2, no. 1, pp. 1-6, 2012.
- [3] Ragesh. N. K, Rajesh R, Anil A.R "Digital image denoising in medical ultrasound images: a survey", *ICGST AIML-11 Conference, Dubai, UAE, 2011*, pp. 6773.
- [4] Rajat Singh and D.S. "Meena; Study of Image Denoising Using Wavelet Transform", Bachelor of Technology Thesis, Department of Computer Science and Engineering National Institute of Technology Rourkela-769008 (ODISHA), 2013.
- [5] R. Sivakumar, "De-noising of Computer Tomography Images using Curve-let transform", *ARPN Journal of Engineering and applied Sciences*, vol. 2, no. 1, pp. 21-26, 2007.
- [6] Anjali Kapoor and Taranjit Singh, "A Brief Review: Speckle Reducing Filtering for Ultrasound Images", *2017 International conference on I-SMAC (IoT in Social, Mobile, Analytics and Cloud)*, pp. 242-246, 2017.

- [7] Hyunho Choi and Jechang Jeong, "Speckle Noise Reduction in Ultrasound Images using SRAD and Guided Filter", 2018 *International Workshop on Advanced Image Technology (IWAIT)*, pp. 1-4, 2018,
- [8] Manoj Diwakar, Sumita Lamba and Himanshu Gupta, "CT Image Denoising Based on Thresholding in Shearlet Domain", *Biomedical & Pharmacology Journal*, vol. 11, no. 2, pp. 671-677, 2018.
- [9] Hyunho Choi, Jechang Jeong, "Speckle noise reduction for ultrasound images by using speckle reducing anisotropic diffusion and Bayes threshold", *J Xray Sci Technol*. Vol. 27, no. 5, pp. 885-898, 2019.
- [10] FaDa Guan , Phuc Ton , ShuaiPing Ge and LiNa Zhao, "Anisotropic diffusion filtering for ultrasound speckle reduction", *Science China Technological Sciences*, vol. 57, no. 3, pp. 607-614, 2014.
- [11] Carlos A Duarte-Salazar, Andrés E Castro-Ospina, Miguel A Becerra, Edilson Delgado-Trejos "Speckle Noise Reduction in Ultrasound Images for Improving the Metrological Evaluation of Biomedical Applications: An Overview", *IEEE Access*, vol. 8, pp. 15983-15999, 2020.
- [12] Milindkumar V. Sarode and Prashant R. Deshmukh, "Reduction of Speckle Noise and Image Enhancement of Images Using Filtering Technique", *International Journal of Advancements in Technology*, vol. 2, no. 1, pp. 30-38, 2011.
- [13] T. Loupas; W.N. McDicken and P.L. Allan, "An adaptive weighted median filter for speckle suppression in medical ultrasonic images", *IEEE Transactions on Circuits and Systems* , vol. 36, no. 1, pp. 129-135, 1989.
- [14] Luis Cadena, Alexander Zotin, Franklin Cadena, Anna Korneeva, Alexander Legalov and Byron Morales; "Noise Reduction Techniques for Processing of Medical Images", *Proceedings of the World Congress on Engineering 2017*, vol I.
- [15] Juan L. Mateo and Antonio Fernandez- Caballero, "Finding out general tendencies in speckle noise reduction in ultrasound images", *Expert systems with Applications*, vol. 36, no. 4, pp. 7786-7797, 2009.
- [16] Yongjian Yu and Scott T. Acton, "Speckle Reducing Anisotropic Diffusion", *IEEE Transactions On Image Processing*, vol. 11, no. 11, pp. 1260-1270, 2002.
- [17] V NagaPrudhviRaj and T Venkateswarlu, "Ultrasound Medical Image Denoising using Hybrid Bilateral Filtering", *International Journal of Computer Applications*, vol. 56, no. 14, pp. 44-51, 2012.
- [18] Hind Oulhaj , Aouatif Amine, Mohammed Rziza and Driss Aboutajdine; "Noise Reduction in Medical Images comparison of noise removal algorithms", 2012 *International Conference on Multimedia Computing and Systems*, pp. 344-349, 2012,
- [19] R.Kumudham, Dhanalakshmi, Aparna Swaminathan, Geetha and Dr. V. Rajendran; "Comparison of The Performance Metrics of Median Filter and Wavelet Filter when applied on Sonar Images for Denoising", 2016 *International Conference on Computation of Power, Energy, Information and Communication (ICCPEIC)*, 2016.
- [20] Di Wu , Xue Du and Kaiyu Wang; "An Effective Approach for Underwater Sonar Image Denoising Based on Sparse Representation", 2018 3rd *IEEE International Conference on Image, Vision and Computing*, 2018.
- [21] Heba Kh., "A Study of Digital Image Fusion Techniques Based on Contrast and Correlation Measures", PhD thesis. Physics Dep., College of Science, Mustansiriyah Univ. 2013.
- [22] Heba Abbas and Sally Ahmad, "Statistical Analysis of Medical Image Fusion Techniques based on Edge Detection", *Advances in Natural and Applied Sciences*, vol. 11, no. 9, pp. 268, 2017.
- [23] Mohammad, A. J., & Hassan, A. K. "Simultaneous Approximation by a New Sequence of Integral Type Based on Two Parameters". *Iraqi Journal of Science*, vol. 62, no. 5, pp. 1666-1674, 2021. <https://doi.org/10.24996/ijs.2021.62.5.29>
- [24] Hesham, M., & Abbas, J. "Multi-criteria Decision Making on the Best Drug for Rheumatoid Arthritis". *Iraqi Journal of Science*, vol. 62, no. 5, pp. 1659-1665, 2021. <https://doi.org/10.24996/ijs.2021.62.5.29>